Theoretical Models of Mercury Dissolution from Dental Amalgams in Neutral and Acidic Flows

RUSSELL G. KEANINI, JACK L. FERRACANE, and TORU OKABE

This article reports an experimental and theoretical investigation of mercury dissolution from dental amalgams immersed in neutral (noncorrosive) and acidic (corrosive) flows. Atomic absorption spectrophotometric measurements of Hg loss indicate that in neutral flow, surface oxide films formed in air prior to immersion persist and effectively suppress significant mercury release. In acidic (pH 1) flows, by contrast, oxide films are unstable and dissolve; depending on the amalgam's material composition, particularly its copper content, two distinct mercury release mechanisms are initiated. In low copper amalgam, high initial mercury release rates are observed and appear to reflect preferential mercury dissolution from unstable Sn_8Hg (γ_2) grains within the amalgam matrix. In high copper amalgam, mercury release rates are initially low, but *increase* with time. Microscopic examination suggests that this feature reflects corrosion of copper from grains of Cu_6Sn_5 (η') and consequent exposure of Ag_2Hg_3 (γ_1) grains; the latter serve as internal mercury release sites and become more numerous as corrosion proceeds. Three theoretical models are proposed in order to explain observed dissolution characteristics. Model I, applicable to high and low copper amalgams in neutral flow, assumes that mercury dissolution is mediated by solid diffusion within the amalgam, and that a thin oxide film persists on the amalgam's surface and lumps diffusive in-film transport into an effective convective boundary condition. Model II, applicable to low copper amalgam in acidic flow, assumes that the amalgam's external oxide film dissolves on a short time scale relative to the experimental observation period; it neglects corrosive suppression of mercury transport. Model III, applicable to high copper amalgam in acidic flow, assumes that internal mercury release sites are created by corrosion of copper in η' grains and that corrosion proceeds *via* an oxidation-reduction reaction involving bound copper and diffusing hydrogen ions. The models appear to capture the correct time dependence of each dissolution mechanism and to provide reasonable fits to the experimental data.

I. INTRODUCTION

ALTHOUGH mercury (Hg) dissolution from dental amalgam has attracted intense research interest, particularly over the last 2 decades, a detailed, quantitative understanding of the process remains elusive. A number of complicating features have slowed progress in this direction: the microstructure of amalgam is complex, typically composed of eight or more distinct metastable phases; in oxygen-containing atmospheres, metal oxides form on the amalgam surface and in intergranular spaces between constituent grains, forming effective, though difficult-to-quantitate barriers to Hg transport; Hg release is sensitive to the external environment and to the amalgam's chemical composition, exhibiting qualitatively distinct, composition-dependent temporal behaviors in neutral and acidic solutions; stress, strain, surface abrasion, microfracture, and corrosion effects on Hg dissolution and solid diffusion remain largely unknown; and the chemistry of solid-phase Hg dissolution and consumption has not been fully characterized.

Traditional low copper amalgam is made by mixing approximately equal weights of Hg and silver-tin alloy powder (composed primarily of Ag_3Sn (γ)) to produce a solid composed primarily of silver-mercury (Ag_2Hg_3 (γ_1)) and tin-mercury (Sn_8Hg (γ_2)) phases.[1] In contrast, high copper amalgam incorporates silver-copper particles either within the silver-tin alloy admixture or within a ternary silver-tin-copper alloy, both of which result in a solid composed primarily of γ_1 and copper-tin (Cu_6Sn_5 (η')) phases when mixed with mercury. It is important to note that the relatively unstable, corrosion-prone γ_2 phase found in low copper amalgam appears in only trace amounts in high copper amalgam; in acidic solutions, this compositional difference leads to qualitatively distinct Hg release characteristics. One of the primary objectives of the present work is to characterize these distinct behaviors experimentally and theoretically.

Surface oxide films and intergranular oxides play a predominant role in both suppressing and determining mercury release mechanisms in dental amalgam.[2,3,4] With regard to intergranular oxides, it is known that relatively thick tin oxide films cover γ_2 grains in low copper amalgam. Thus, Hg release from both low and high copper amalgam in oxygen-containing and neutral aqueous environments appears to originate from γ_1 grains within the matrix. Important insight into the composition, structure, and thickness of surface oxide films was recently obtained by Hanawa et al.,[2] who used argon-ion sputtering to study oxide films formed in oxygen-rich, aqueous, and saline solutions. This and related work[3,4] demonstrate that surface films form relatively quickly in oxygen-containing atmospheres (within an hour of initial exposure), that Hg concentration varies

RUSSELL G. KEANINI, Associate Professor, is with the Department of Mechanical Engineering and Engineering Science, University of North Carolina at Charlotte, Charlotte, NC 28223. JACK L. FERRACANE, Professor, is with the Department of Biomaterials and Biomechanics, School of Dentistry, Oregon Health Sciences University, Portland, OR 97201-3007. TORU OKABE, Regents Professor and Chairman, is with the Department of Biomaterials Science, Baylor College of Dentistry, Dallas, TX 75246.
Manuscript submitted August 8, 2000.

spatially and assumes a non-negligible magnitude at the film's surface, and that Hg accumulates within and immediately below the surface oxide film. These observations provide the basis for constructing a model of Hg release from oxide film-covered amalgam immersed in either air or neutral solutions.

While the presence of oxides generally inhibits mercury dissolution, corrosion can enhance the dissolution process through at least three mechanisms. In the first, the typically slow phase transformation from γ_1 (Ag$_2$Hg$_3$) to β_1 (Ag$_9$Hg$_{11}$) is accelerated by corrosion; due to the lower (relative) Hg content of β_1, accelerated Hg loss is implied.[1] The second and third mechanisms, which are experimentally and theoretically investigated here, occur in acidic (pH 1) environments. In both cases, tin oxide films are unstable and dissolve rapidly. In low copper amalgam, mercury within unstable γ_2 grains then also begins to dissolve. Due to the prevalence of the γ_2 phase, initial Hg release rates are high; however, as Hg from the γ_2 phase depletes itself and, as insoluble corrosion products accumulate around γ_2 grains, mercury release decays. In high copper amalgam, the copper in the Cu$_6$Sn$_5$ (η') phase is more prone to dissolution than in either of the Hg-containing phases (γ_1 and, to a limited extent, γ_2) and thus dissolves first.[5] However, dissolution of the copper-tin phase effectively exposes the surface of neighboring γ_1 grains and, in the process, creates internal sites for Hg release. In this case, mercury dissolution actually *increases* with time. This article presents experimental evidence suggesting the existence of these latter mechanisms. Significantly, models applicable to low and high copper alloys immersed in either neutral or acidic flows are developed to explain observed mercury release characteristics.

II. MODELS OF DYNAMIC MERCURY DISSOLUTION IN FLUID FLOWS

A. *Model I: Hg Dissolution from Low and High Cu Amalgam in Neutral Flow*

Here, a tin oxide layer that forms in air prior to immersion persists within the flow.[4,6] We assume that the oxide layer thickness remains fixed, or equivalently, that the time scale for continued film growth within the flow is much larger than the duration of the experiment. This assumption is consistent with Marek and Su,[4] who found that oxide film formation is characterized by two physical processes and two corresponding time scales: monolayer nucleation and growth, which takes place on a fast, pH-dependent time scale ranging from 1 to 10 seconds, and formation of the quasistatic three-dimensional film, which occurs on a slow time scale ranging from $\approx$10 minutes to $\approx$1 hour. We also assume that due to the film's thinness,[2] which is on the order of 5 to 10 nm, mercury concentration decreases linearly across the film. In reality, as found by Hanawa *et al.*,[2] subsurface mercury concentration exhibits a depthwise, oscillatory variation about a slowly varying mean; the mean concentration profile increases with depth toward an asymptotic value, C_∞, and maximum oscillation amplitudes are approximately 20 to 25 pct of C_∞ (where oscillations are completely damped within $\approx$5 to 10 nm of the surface). To a first order of approximation, we neglect these spatial oscillations and model the mean concentration profile.

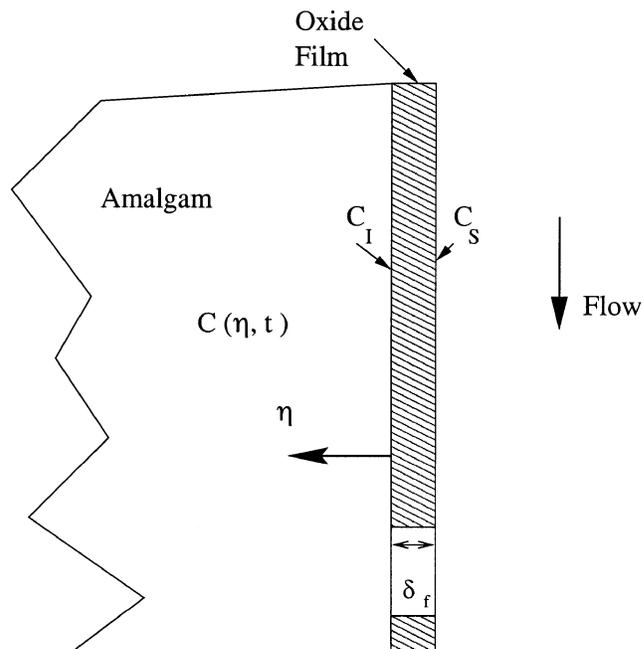A schematic of the modeled problem is shown in Figure

Fig. 1—Problem definition for model I.

1. The equation governing diffusion of mercury within both the amalgam and the oxide film is given by

$$\frac{\partial C}{\partial t} = D_\alpha \frac{\partial^2 C}{\partial \eta^2} \qquad [1]$$

where $C = C(\eta,t) = [\text{Hg}]|(\eta,t)$ is the concentration of mercury, D_α is the diffusivity of mercury in amalgam ($\alpha = m$) or oxide film ($\alpha = f$), η is the coordinate normal to the film-solution interface, and t is time. Note that all three models described in this article assume that the time scale for mercury dissolution within the amalgam is short relative to the diffusion time scale. This assumption rests on Hanawa's[2] observation that Hg concentration gradients exist within amalgam; if dissolution were slow relative to diffusion, concentration gradients would not be observed. The boundary conditions and initial condition on Eq. [1] are as follows. Since mass cannot accumulate at the amalgam-oxide film interface ($\eta = 0$), the mass flux of mercury from the unoxidized amalgam must equal the mercury mass flux into the oxide film. Thus,

$$D_m \frac{\partial C}{\partial \eta} = D_f \frac{\partial C}{\partial \eta} \qquad \eta = 0, t \geq 0 \qquad [2]$$

At locations well removed from the amalgam-oxide interface and for experimental times much shorter than L^2 / D_m (where L is the amalgam thickness), mercury concentration remains fixed at its nominal initial value, C_∞. Thus,

$$C \rightarrow C_\infty \text{ as } \eta \rightarrow \infty \qquad [3]$$

Finally, we assume that the initial mercury concentration is spatially uniform and equal to C_∞:

$$C = C_\infty \quad t = 0, \eta \geq 0 \qquad [4]$$

In order to state the boundary value problem given by Eqs. [1] through [4] in a more convenient form, we re-express the flux balance at the amalgam-oxide film interface

$\eta = 0$ (given by Eq. [2]) in the *form* of a convective mass-transfer boundary condition:

$$D_m \frac{\partial C}{\partial \eta} = h_m (C - C_o) \qquad [5]$$

where h_m is an effective convective mass transfer coefficient and C_o is a constant effective mass concentration. In order to express h_m and C_o in terms of known or measurable quantities, we first express $C(\eta, t)$ within the film as

$$C(\eta,t) = \frac{[C_I(t) - C_S(t)]}{\delta_f} \eta + C_I(t) \qquad [6]$$

where $C_I(t) = C(0, t)$ is the Hg concentration at the amalgam-film interface, $C_S(t) = C(-\delta_f, t)$ is the Hg concentration at t0he film-solution interface, and δ_f is the (constant) film thickness. We then integrate Eqs. [6] across the film and solve for $C_S(t)$:

$$C_S(t) = \frac{M_o}{\delta_f} - C_I(t) \qquad [7]$$

where $M_o = (C_I + C_S)\delta_f$, a constant equal to twice the total (area averaged) mass of Hg within the film. Equation [7] expresses the fact that as t increases and C_I decreases, C_S increases; as C_I and C_S approach a common value, $\frac{\partial C}{\partial \eta}$ becomes small and Hg transport across the film becomes vanishingly small. (In order to prove that M_o is constant, we first note that, due to the assumed linear concentration profile across the film, $\frac{\partial^2 C}{\partial \eta^2} = 0$. Thus, from the diffusion equation, $\frac{\partial C}{\partial t}$ also equals zero, implying that

$$\int_{-\delta_f}^{0} \frac{\partial C}{\partial t} d\eta = \frac{\partial}{\partial t} \int_{-\delta_f}^{0} C d\eta = 0 \qquad [8]$$

Substituting Eq. [6] for $C(\eta, t)$ in the second integral, we obtain

$$\frac{\partial M_o}{\partial t} = 0$$

completing the proof.) Finally, replacing C_S in Eq. [6] with the right side of Eq. [7] and inserting the result into Eq. [2] yields

$$D_m \frac{\partial C}{\partial \eta} = \frac{2D_f}{\delta_f} C - \frac{D_f M_o}{\delta_f^2} \quad \eta = 0, t \geq 0 \qquad [9]$$

where, for clarity, $C_I(t)$ has been replaced with C (since $C_I(t) = C(0,t)$). Thus, comparing Eq. [9] with Eq. [5], we see that

$$h_m = \frac{2D_f}{\delta_f} \text{ and } C_o = \frac{M_o}{2\delta_f} = \frac{C_I + C_S}{2} \qquad [10]$$

The solution is obtained by defining V as

$$V = C - C_o \qquad [11]$$

Based on this definition, the problem becomes

$$\frac{\partial V}{\partial t} = D_m \frac{\partial^2 V}{\partial \eta^2} \qquad [12]$$

$$\frac{\partial V}{\partial \eta} = hV \quad \eta = 0, t \geq 0 \qquad [13]$$

$$V \to V_\infty \text{ as } \eta \to \infty \qquad [14]$$

$$V = V_\infty \quad t = 0, \eta \geq 0 \qquad [15]$$

where $h = h_m/D_m$ and $V_\infty = C_\infty - C_o$. The solution to Eqs. [12] through [15] is given by[7]

$$V(\eta,t) = V_\infty \left[\text{erf}\left(\frac{\eta}{2\sqrt{D_m t}}\right) + \exp\left[h\eta + h^2 D_m t\right] \text{erfc}\left[\frac{\eta}{2\sqrt{D_m t}} + h\sqrt{D_m t}\right] \right] \qquad [16]$$

where erf (η) and erfc (η) are the error function and the complimentary error function, respectively.

Given $V(\eta, t)$, the mass flux, $\dot{m}_{Hg}$, of mercury from the amalgam into the flowing solution is given by

$$\dot{m}_{Hg} = D_m \frac{\partial V}{\partial \eta}\Big|_{\eta=0,t}$$

$$= h_m(C_\infty - C_o) \exp(h^2 D_m t) \text{er f c}(h\sqrt{D_m t}) \qquad [17]$$

B. *Model II: Hg Dissolution from Low-Cu Amalgam in Acidic (pH 1) Flows*

Since oxide films (comprised primarily of SnO_2) are unstable at pH 1, we assume that the oxide film dissolves on a time scale much shorter than that of the experiment's duration. Marek's[8] results, which show an order of magnitude increase in Hg dissolution rate when air-aged amalgam is immersed in pH 1 solution, suggest that the oxide film dissolves on a time scale shorter than 2 h; likewise, our results (discussed in Section IV) indicate that the film dissolves on a time scale on the order of 1 hour. Thus, referring to Figure 1, we assume that the surface oxide film is absent and we focus attention on the region $\eta \geq 0$. We also neglect corrosion-induced suppression of Hg release. A scanning electron microscope (SEM) examination of low copper amalgam suggests that buildup of corrosion products is minimal after 6 days of immersion (*i.e.*, the experimental observation period). Based on initially high dissolution rates, we also assume that dissolution-prone surface Hg atoms are quickly depleted (*i.e.*, within the first 3 or 4 hours of immersion) and that surface Hg concentration then assumes a constant, possibly near-zero, magnitude, $C(\eta = 0, t) = C_f$. This assumption appears to be consistent with previous work,[2] which indicates that surface mercury concentration assumes a relatively fixed magnitude in water and air. However, equivalent data is not available concerning surface characteristics in acidic environments. It should be noted that use of a convective boundary condition at $\eta = 0$ leads to an extremely poor fit between theory and experiment.

Defining V as

$$V(\eta,t) = C(\eta,t) - C_f \qquad [18]$$

and noting that the governing equation, far-field boundary condition, and initial condition given by Eqs. [1], [3], and [4], respectively, remain unchanged, we obtain the corresponding transformed equations in Eqs. [12], [14], and [15]. (Note, however, that V is now given by Eq. [18].) The boundary condition in Eq. [2] is replaced, however, by

$$V = 0 \quad \eta = 0, \quad t \geq 0 \qquad [19]$$

The solution[7] is given by

$$V(\eta,t) = V_\infty \, \mathrm{erf}\left(\frac{\eta}{2\sqrt{D_m t}}\right) \qquad [20]$$

where $V_\infty = C_\infty - C_f$. The corresponding mass flux is given by

$$\dot{m}_{Hg} = D_m \frac{\partial V}{\partial \eta}\Big|_{\eta=0,t} = (C_\infty - C_f)\sqrt{\frac{D_m}{\pi}}\, t^{-1/2} \qquad [21]$$

C. *Model III: Hg Release from High-Cu Amalgam in Acidic (pH 1) Flows*

Based on microscopic evidence, corrosion in high-Cu samples occurs both on the amalgam's surface and at interior locations. Since copper in the η' copper-tin phase (Cu_6Sn_5) is preferentially dissolved at this pH,[5] new interior dissolution sites, corresponding to exposed γ_1 (Ag_2Hg_3) grains, are likely created when copper begins to dissolve. In order to model Hg release in this case, it is necessary to model the surface and internal corrosion processes first. In turn, we must relate corrosion to the rate of creation of internal Hg dissolution sites. Finally, given the rate of dissolution site creation, we must model subsequent internal Hg transport to the amalgam's surface.

The model's assumptions are as follows.

(1) Based on experimental observations, corrosion begins on the amalgam's surface and proceeds inward. As corrosion continues, intergranular spacing increases, suggesting that resistance to Hg transport within the corroded region (*i.e.*, from internally exposed dissolution sites to the flowing external solution) is relatively small. We thus assume that the effective diffusivity within corroded amalgam is much greater than mercury's diffusivity in noncorroded solid amalgam. Equivalently, we assume that internally dissolved Hg does not accumulate within corroded amalgam and, moreover, that the concentration of dissolved Hg within corroded amalgam is small relative to C_∞ (where again C_∞ is the initial solid phase mercury concentration).

(2) Corrosion, and associated creation of internal mercury dissolution sites, depends only on time t and on depth η below the amalgam surface.

(3) The concentration of bound Hg at each internal release site remains fixed at its nominal initial value (C_∞). Since initial Hg concentration is on the order of 47 wt pct, and since Hg loss is estimated to reduce C_∞ by no more than 0.001 pct over the 6-day observation period (based on observed Hg loss rates described subsequently), this assumption is clearly reasonable.

Based on the first three assumptions, we express the local instantaneous rate of internal Hg dissolution as
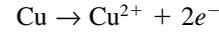
$$\Delta \dot{m}_{Hg} = h_i C_\infty \Delta A(\eta,t) \qquad [22]$$

where h_i is the mass transfer coefficient for interior Hg release sites and $\Delta A(\eta,t)$ is the local exposed area created by copper corrosion.
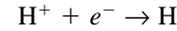
(4) The coefficient h_i is constant. Since h_i generally depends on the concentration difference $\Delta C = C_\infty - C_l$, between

bound mercury (C_∞) and mercury in solution (C_l), this assumption presumes that ΔC remains fixed; given that C_l is much smaller than 1 pct while C_∞ remains essentially constant (as previously noted), then again, this assumption appears reasonable.

(5) Copper corrosion occurs by an oxidation-reduction reaction[9] in which copper is oxidized according to

$$Cu \rightarrow Cu^{2+} + 2e^-$$

and diffusing hydrogen ions are reduced according to

$$H^+ + e^- \rightarrow H$$

Although corrosion, and particularly subsurface corrosion, remains poorly understood,[10] this assumption presumes that relatively mobile hydrogen ions diffuse into amalgam and oxidize the most unstable constituent; the assumption is also consistent with, and explains, subsurface corrosion.

(6) The local, instantaneous rate of volume loss from the amalgam due to corrosion is proportional to the local rate of copper corrosion:

$$\frac{\partial V(\eta,t)}{\partial t} = c_1 \frac{\partial [Cu^{++}]|_{(\eta,t)}}{\partial t} \qquad [23]$$

where c_1 is a constant of proportionality.

(7) As copper corrosion occurs, a new area for Hg dissolution is created. We assume that the local instantaneous rate of area creation is proportional to the rate of volume loss given in Eq. [23]:

$$\frac{\partial A(\eta,t)}{\partial t} = c_2 \frac{\partial V(\eta,t)}{\partial t} \qquad [24]$$

where again c_2 is a constant of proportionality. This assumption is based on the expectation that local volume loss corresponds to corrosive removal of monolayers at each corrosion site. Thus, for a given characteristic monolayer thickness d_m, $c_2 \approx d_m^{-1}$.

(8) The kinetics for copper corrosion depend on the local instantaneous concentrations of unreacted copper and hydrogen ions:

$$\frac{\partial}{\partial t}[Cu^{++}]|_{(\eta,t)} = K_c[Cu]|_{(\eta,t)}[H^+]^n|_{(\eta,t)} \qquad [25]$$

where K_c is the reaction rate constant and n is a constant. Although it is presumed that $n = 2$, we leave the equation in this more general form.

(9) As in model II, the surface oxide film dissolves on a time scale that is short relative to the experimental time scale.

We envision copper corrosion and the associated creation of Hg dissolution sites as occurring at depth-varying rates, as shown in Figure 2. From the figure we obtain the following expression for the total amount of Hg released by dissolution at time t:

$$\dot{m}_{Hg} = h_i \Delta A(\eta_0,t)[C(\eta_0,t) - C^l(\eta_0,t)] + h_i \Delta A(\eta_1,t)[C(\eta_1,t)$$
$$- C^l(\eta_1,t)] + \ldots h_i \Delta A(\eta_N,t)[C(\eta_N,t) - C^l(\eta_N,t)] + \dot{m}_0$$

where $\Delta A(\eta_i,t)$ is the area of amalgam exposed by corrosion between depths η_i and η_{i+1} (at time t); $C(\eta_i,t)$ and $C^l(\eta_i,t)$ are the corresponding concentrations of bound and free Hg;
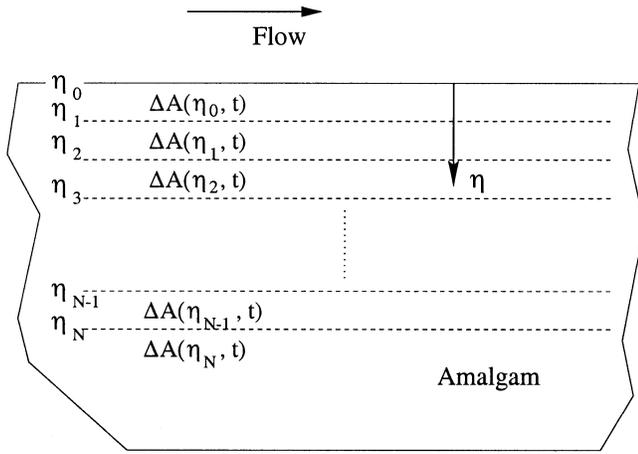
Fig. 2—Problem definition for model III.

and $\dot{m}_0$ is the initial Hg dissolution rate extant prior to corrosion onset. Introducing the first, third, and fourth assumptions and allowing $N \rightarrow \infty$, the summation above becomes

$$\dot{m}_{Hg} = h_i C_\infty \int_0^{\delta_c(t)} dA + \dot{m}_0 \qquad [26]$$

where $\delta_c(t)$ is the time-varying depth of the corrosion zone (below the amalgam's surface). Noting that at time t,

$$dA = -\frac{\partial A}{\partial \eta} d\eta \qquad [27]$$

and that for $\eta > \delta_c(t)$, $A(\eta,t) = 0$, we express the integral in Eq. [26] as

$$\dot{m}_{Hg}(t) = -h_i C_\infty \int_0^\infty \frac{\partial A}{\partial \eta} d\eta + \dot{m}_0 \qquad [28]$$

(The negative sign on the right side of Eq. [27] is required in order to ensure positive dA.) Now, based on the first, sixth, seventh, and eighth assumptions, the local rate of area creation can be related to the local concentration of hydrogen ions as

$$\frac{\partial A}{\partial t} = c_3 [H^+]^n \qquad [29]$$

where c_3 is a positive constant. Thus, the instantaneous exposed area at depth η can be expressed as

$$A(\eta,t) = \int_0^t \frac{\partial A}{\partial t} \Big|_{(\eta,t)} dt = c_3 \int_0^t [H^+]^n \Big|_{(\eta,t)} dt \qquad [30]$$

Differentiating the last expression with respect to η and inserting the result into Eq. [28], we obtain

$$\dot{m}_{Hg}(t) = -c_3 h_i C_\infty \int_0^\infty \left[\frac{\partial}{\partial \eta} \int_0^t [H^+]^n dt \right] d\eta + \dot{m}_0 \qquad [31]$$

which upon rearrangement becomes

$$\dot{m}_{Hg}(t) = -c_3 h_i C_\infty \int_0^t \left[\int_0^\infty \frac{\partial}{\partial \eta} [H^+]^n d\eta \right] dt + \dot{m}_0 \qquad [32]$$

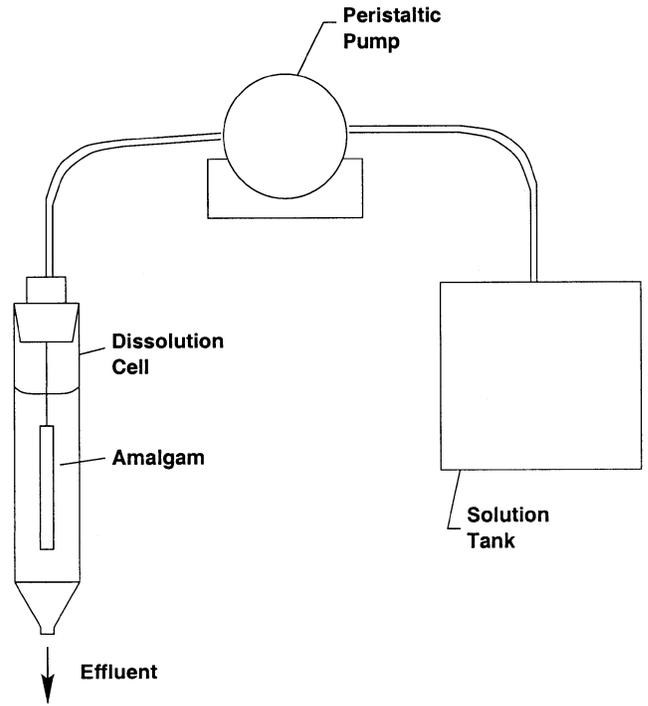Fig. 3—Schematic of experimental setup.

or

$$\dot{m}_{Hg}(t) = -c_3 h_i C_\infty \int_0^t \left[[H^+]^n \big|_{(\infty,t)} - [H^+]^n \big|_{(0,t)} \right] dt + \dot{m}_0 \qquad [33]$$

As shown in the Appendix,

$$[H^+] \big|_{(\eta,t)} = [H_o^+] \mathrm{erfc} \left(\frac{\eta}{2\sqrt{D_H t}} \right) \qquad [34]$$

where $[H]_o^+$ is the concentration of $[H^+]$ in the flowing solution and thus the concentration at the amalgam's surface, and where D_H is the diffusion coefficient for H^+ within amalgam. (The mass transfer Peclet number, which indicates the relative importance of convective-to-diffusive mass transfer within the flowing solution, is small in our experiments. Thus, the concentration of $[H^+]$ at the amalgam's surface is essentially equal to the bulk concentration of $[H^+]$ within the flow.) Thus, since $[H^+] \big|_{(O,t)} = [H_o^+]$ [erfc(0) = 1] and $[H^+] \big|_{(\infty,t)} = 0$ [$erfc(\infty) = 0$], we find that $\dot{m}_{Hg}$ increases linearly with time

$$\dot{m}_{Hg}(t) = c_4 t + \dot{m}_0 \qquad [35]$$

where $c_4 = c_3 h_i C_\infty [H_o^+]^n$ is a positive constant.

III. EXPERIMENTAL PROCEDURES

Commercial low copper (Velvalloy) and high copper (Dispersalloy) amalgams were prepared according to ANSI/ADA Specification No. 1. Triturated specimen were compressed to 14 MPa in a steel die, resulting in test specimen having dimensions of $3 \times 3 \times 25$ mm and nominal mercury concentrations of 47 pct. Subsequently, specimen were aged in room air for 3 days prior to dissolution testing. Dissolution tests were run for 144 hours (6 days) using the experimental setup depicted in Figure 3. In each test, specimen were placed

in each of four stoppered dissolution cells and immersed continuously in slowly moving deionized water or pH 1 solution. Deionized water provides an approximate analog for the flow of saliva over amalgams while the pH 1 solution simulates conditions believed to exist in crevices and pits on corroding in-service amalgam.[8] In order to suppress adsorption of mercury ions within the test apparatus, nitric acid (HNO_3, 10 wt pct concentration) was added to the test solution (within the test solution tank). Flow rates through each dissolution cell were fixed at 0.075 mL/min throughout the experimental period, and effluent from each cell was sampled nine times; the first three samples were gathered at 1.5, 3, and 4.5 hours following the start of any given experiment ($t = 0$), and the remaining six were taken at 24-hour intervals following $t = 0$. The concentration of mercury in each sample was determined by the cold vapor atomic absorption spectrophotometry technique and test specimen were examined at the conclusion of each experiment using scanning electron microscopy.

IV. RESULTS AND DISCUSSION

Model I predicts that Hg dissolution from high and low copper amalgam in neutral flow has a somewhat complicated time dependence (Eq. [17]), while models II and III, applicable to low and high copper amalgam in acidic flow, predict that $\dot{m}_{Hg} \propto t^{-1/2}$ and $\dot{m}_{Hg} \propto t$, respectively (Eqs. [21] and [35]). Equations [17] and [35] each contain two independent parameters, a_I and b_I, and a_{III} and b_{III}, respectively, where $a_I = h_m(C_\infty - C_o)$, $b_I = h\sqrt{D_m}$, $a_{III} = c_4$, and $b_{III} = \dot{m}_o$. Likewise, Eq. [21] contains a single parameter, $a_{II} = (C_\infty - C_f)\sqrt{D_m/\pi}$. The parameters a_I and b_I are determined by nonlinear least-squares fitting while a_{II}, a_{III}, and b_{III} are determined using linear least-square fits. In each case, a chi-square merit function, $\chi^2 = \chi^2(\mathbf{t}; \mathbf{a}_\alpha)$, given by

$$\chi^2 = \sum_{i=1}^{N} \left[\frac{\dot{m}_i - \dot{m}(t_i; \mathbf{a}_\alpha)}{\sigma_i} \right]^2 \qquad [36]$$

is minimized with respect to each parameter vector $\mathbf{a_I} = [a_I, b_I]$, $\mathbf{a_{II}} = [a_{II}]$, and $\mathbf{a_{III}} = [a_{III}, b_{III}]$. Here, $\mathbf{t} = t_i$ is the vector of experimental measurement times, $\dot{m}_i$ is the measured Hg dissolution rate at time t_i, σ_i is the uncertainty in the ith dissolution rate measurement, and $N = 9$. Since errors σ_i in each mass loss measurement are unknown, these are taken as 1.[11] Calculated values of each parameter are given in Table I. Coefficients of determination, R^2, are calculated for models II and III. (Since model I cannot be expressed in linear form, R^2 is not calculated in this case.) This quantity gives the proportion of variance in mercury dissolution rate that is explained by the regression line and thus provides a measure of how well the regression line predicts observed loss rates. The formula for R^2 is given by
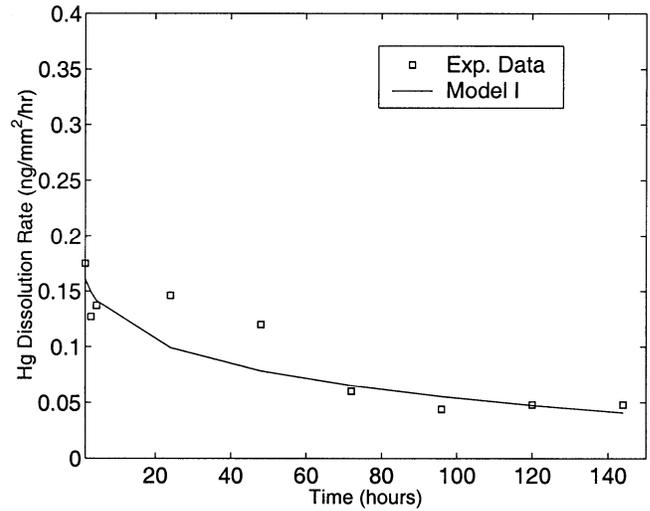

Fig. 4—Experimental and theoretical mercury dissolution rates for low copper amalgam in neutral flow.
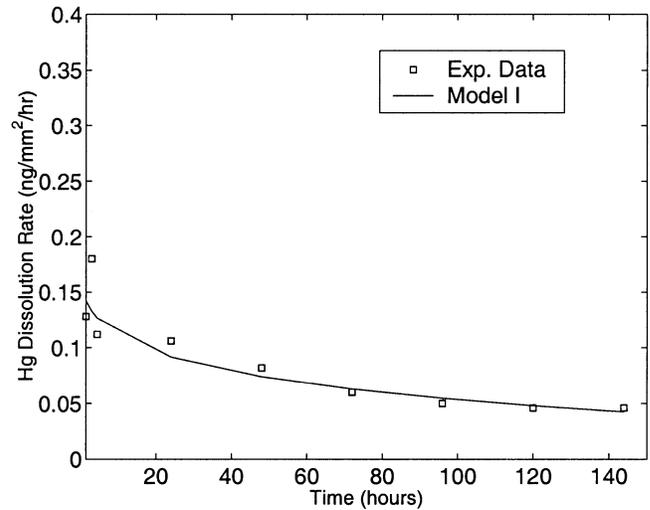

Fig. 5—Experimental and theoretical mercury dissolution rates for high copper amalgam in neutral flow.

$$R^2 = 1 - \frac{\sum_{i=1}^{N} (\dot{m}_i - \hat{\dot{m}}_i)^2}{\sum_{i=1}^{N} (\dot{m}_i - \overline{\dot{m}})^2} \qquad [37]$$

where $\dot{m}_i$ is again the Hg dissolution rate observed at time t_i, $\hat{\dot{m}}_i$ is the corresponding dissolution rate calculated *via* the regression line, N is the number of observations, and $\overline{\dot{m}}$ is the mean dissolution rate for the experiment. Values for R^2 are given in Table I.

Time-dependent mercury release from both low and high copper amalgams in neutral flow is consistent with that predicted by model I (Figures 4 and 5). In both cases, the rate of mercury release is initially high, but then decays in a more or less monotonic fashion through the remainder of the six-day observation period. The data in Figures 4 and 5 suggest that spatially oscillatory mercury accumulations, which are trapped within and immediately below the surface oxide film during film formation,[2] diffuse into the external flow throughout the experiment. This interpretation is suggested first by the observation that Hg dissolution rates
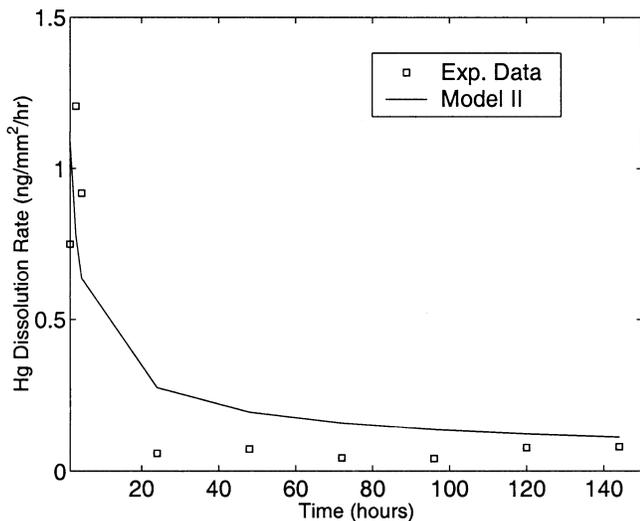
Fig. 6—Experimental and theoretical mercury dissolution rates for low copper amalgam in acidic (pH 1) flow.

Fig. 7—Experimental and theoretical mercury dissolution rates for high copper amalgam in acidic (pH 1) flow.

increase, or are above predicted rates during the first 60 to 70 hours of immersion (Figures 4 and 5). This period of relatively high loss appears to reflect dissolution of large in-film Hg accumulations.[2] Second, subsequent dissolution rates oscillate about the monotonically decaying theoretical curves, indicating passage of smaller, oscillatory, subfilm mercury accumulations. As an aside, we note that a number of other explanations for oscillatory dissolution appear to be less likely. For example, chemical thinning of the oxide film is argued against since oxide films are stable in water.[8] Similarly, enhanced mercury release due to film abrasion, possibly produced during specimen transfer to the dissolution cells, appears unlikely since mercury release decays *monotonically* when freshly abraded amalgam is placed in water;[4] the decay in this case occurs on a time scale of an hour or less and reflects rapid oxide film formation. Oscillatory mercury release over tens of hours is clearly inconsistent with this mechanism. Oscillatory dissolution produced by time-dependent temperature variations also appears unlikely since the experiments were performed on different weeks.

Experimental and theoretical Hg dissolution rates from low copper amalgam immersed in acidic (pH 1) flow are compared in Figure 6. The most noteworthy feature, which provides key insight into the underlying mercury release mechanism, concerns the short period of high Hg loss observed during the first 90 minutes of immersion. In particular, the transient appears to be initiated by rapid oxide film loss at the amalgam's surface and is likely produced by subsequent Hg dissolution from unstable γ_2 (Sn$_8$Hg) grains within the exposed matrix. This interpretation rests on the premises that oxide film dissolution occurs within the first hour (approximately) of immersion and that the amount of Hg released from the dissolving oxide film is small compared to the amount released from underlying γ_2 grains. With regard to the first premise, as mentioned, Marek's[8] observations suggest a film dissolution time scale of 2 hours or less (where 2 hours is the time resolution of his measurements). More to the point, our results, which show 90-minute postimmersion Hg loss rates that are approximately an order of magnitude higher than those in neutral flow (Figures 4 and
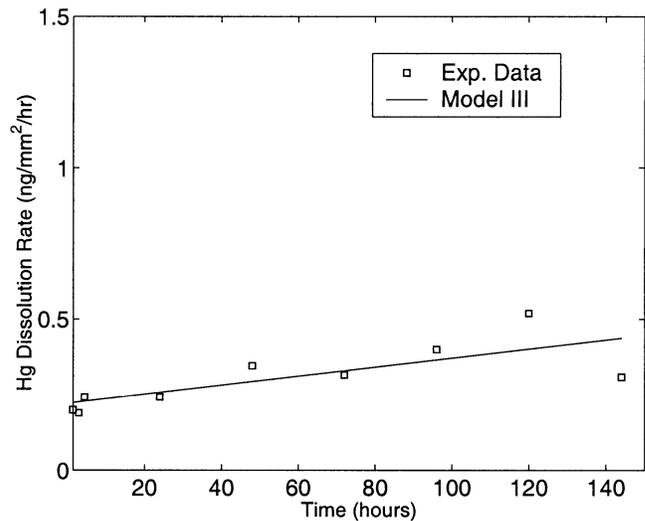
5), indicate significant oxide film loss on a time scale of 90 minutes or less. With regard to the second premise, since oxide film thicknesses and the amount of Hg trapped within oxide films are essentially independent of the amalgam's composition,[2] and since a transient is *not* observed when *high copper* amalgam is immersed in acid (Figure 7), then it is apparent that only small amounts of Hg are released by film dissolution. Thus, we argue that corrosive Hg release from low copper amalgam is produced predominantly by dissolution from unstable γ_2 grains, exposed by rapid surface oxide film loss.

The rapid decay in dissolution rate observed between $t = 1.5$ h and $t = 24$ h in Figure 6 appears to reflect mercury depletion from near-surface γ_2 grains, rather than suppression due to corrosion product buildup. This interpretation is suggested by SEM micrographs, which show negligible corrosion product buildup after 6 days of immersion. (Significant corrosion product buildup *is* observed after 30 days of immersion.) As shown in Figure 6, Model II overpredicts release rates through most of the experiment; nevertheless, qualitative features of post immersion mercury release appear to be adequately captured. Since the model assumes that the oxide film is completely dissolved throughout the observation period and since this assumption is only valid for $t \gtrsim 2$ h an improved model would focus on processes (*e.g.*, film dissolution and time-dependent exposure of γ_2 grains) occurring during the first few hours of immersion. Finally, we note that for $t \gtrsim 20$ h, the loss rate is slightly oscillatory, having a period of approximately 60 to 70 hours. As in the first two sets of experiments (Figures 4 and 5), this feature appears to reflect passage of the spatially oscillatory Hg concentration profile.

Mercury dissolution from high copper amalgam in acidic flow exhibits significant qualitative differences from that observed in acid-immersed low copper amalgam (Figures 6 and 7). As shown in Figure 7, the Hg dissolution rate increases at a nominally linear rate throughout the observation period; indeed, the dissolution rate maintains a linear rate of increase over an entire month (result not shown). As discussed above, SEM micrographs indicate the occurrence of surface and subsurface corrosion; again, Espevik's[5] work

indicates that following initial oxide film dissolution (during the first 1 or 2 hours of immersion), copper in the η' (Cu$_6$Sn$_5$) phase dissolves and, in the process, exposes Ag$_2$Hg$_3$(γ_1) grains within the matrix. These then serve as new mercury dissolution sites. Due to the relative stability of γ_1 grains, the initial dissolution rate from high Cu amalgam (for $t \leq$ 4.5 h) is almost an order of magnitude smaller than the initial rate from acid-immersed low copper amalgam (Figure 6). As argued previously, the latter result reflects the relative instability of γ_2 (Sn$_8$Hg) in low pH solutions. Once again, we observe that the dissolution rate oscillates about the theoretical curve and, again, interpret this as reflecting diffusional transport of the spatially varying, subsurface Hg concentration profile.

V. SUMMARY AND CONCLUSIONS

Three models of mercury dissolution from dental amalgam immersed in neutral and acidic flows have been proposed. The models capture observed dissolution characteristics and provide a basis for interpreting experimental observations. Model I, applicable to low and high copper amalgam immersed in neutral flow, assumes that surface oxide films are unaffected by immersion (on the experimental time scale) and lumps diffusive transport across the film into an effective convective boundary condition. Model II, which applies to dissolution from low copper amalgam in acidic (pH 1) flow, assumes that surface oxide films dissolve on a time scale that is short relative to the experimental observation period and that neglects the effect of corrosion-product buildup. Model III applies to high copper amalgam in acidic flow and introduces the following assumptions: (1) initially, copper in the η' (Cu$_6$Sn$_5$) phase dissolves by an oxidation-reduction reaction involving diffusing hydrogen ions and bound copper; (2) copper corrosion exposes γ_1 (Ag$_2$Hg$_3$) grains which then serve as internal (and surface) mercury dissolution sites; (3) the rate of internal dissolution site creation is proportional to the rate of copper corrosion (which in turn is proportional to some power of the local hydrogen ion concentration); and (4) accumulation of dissolved mercury within corroded amalgam is negligible. Based on these and on other assumptions described above, an expression for the time- and position-dependent rate of mercury dissolution is derived and is used to determine the total instantaneous Hg dissolution rate. Mercury dissolution rates appear to oscillate relative to predicted rates; it is not clear, however, whether the apparent oscillations reflect diffusive transport of accumulated, spatially oscillatory, subsurface mercury or undetermined random processes. This feature is currently under investigation.

ACKNOWLEDGMENTS

LIST OF SYMBOLS

$\mathbf{a}_P$	parameter vector for model P
A	area
C	mercury concentration
D	solid-phase diffusivity
D_f	Hg diffusivity in oxide film
D_H	diffusivity of hydrogen ions in amalgam
D_m	Hg diffusivity in unoxidized amalgam
h	convective mass-transfer coefficient
h_i	convective mass-transfer coefficient for internal dissolution sites
$\dot{m}_{Hg}$	total mercury dissolution rate per unit area of amalgam
m_0	initial Hg dissolution rate (per unit area of amalgam)
$[M]$	concentration of species M
M_o	2 times area-averaged mass of mercury in oxide film
t	time

Greek Letters

δ_f	oxide film thickness
ΔA	internal differential area for dissolution of Hg
η	inward directed normal coordinate
σ_i	uncertainty in ith dissolution rate measurement
χ^2	chi-square merit function

APPENDIX

The initial value problem governing diffusion of hydrogen ions in solid amalgam is defined by

$$\frac{\partial H}{\partial t} = D_H \frac{\partial^2 H}{\partial \eta^2} \qquad [A1]$$

$$H = H_0 \ \eta = 0, \ t \geq 0 \qquad [A2]$$

$$H \to 0 \text{ as } \eta \to \infty, \ t \geq 0 \qquad [A3]$$

$$H = 0 \ t = 0, \ \eta \geq 0 \qquad [A4]$$

where $H_o = [H_o^+]$ is the concentration of H^+ in the flowing solution, $H = [H^+]$ is the local concentration of H^+ within the amalgam, D_H is the corresponding solid phase diffusivity, and where we assume that the concentration of H^+ within amalgam is zero prior to immersion in the acidic flow.

The solution is given by[7]

$$H(\eta,t) = [H_0^+] \operatorname{erfc}\left(\frac{\eta}{2\sqrt{D_H t}}\right) \qquad [A5]$$

REFERENCES

1. S.J. Marshall and G.W. Marshall: *Adv. Dental Res.*, 1992 vol. 6, pp. 94-99.
2. T. Hanawa, H. Takahashi, M. Ota, R.F. Pinizzoto, J.L. Ferracane, and T. Okabe: *J. Dental Res.*, 1987, vol. 66, pp. 1470-78.
3. J.L. Ferracane, T. Nguyen, T. Hanawa, and T. Okabe: *J. Dental Res.*, 1988, vol. 67, pp. 117-23.
4. M. Marek and Y.Y. Su: *Proc. Int. Assoc. Dental Res.*, 1997, Abs. 3123.
5. S. Espevik: *Scand. J. Dental Res.*, 1977, vol. 85, pp. 631-36.
6. T. Okabe, J.L. Ferracane, C. Cooper, H. Matsumoto, and M. Wagner: *J. Dental Res.*, 1987, vol. 66, pp. 33-37.
7. H.D. Carslaw and J.C. Jaeger: *Conduction of Heat in Solids*, Oxford, New York, NY, 1959, pp. 59-72.
8. M. Marek: *J. Dental Res.*, 1997, vol. 76, pp. 1308-15.
9. D.J. Duquette: *Intermetallic Compounds: Vol. 1, Principles*, J.H. Westbrook and R.L. Fleischer, eds., Wiley, New York, NY, 1994.
10. M. Marek: *Adv. Dental Res.*, 1992, vol. 6, pp. 100-09.
11. W.H. Press, S.A. Teukolsky, W.T. Vetterling, and B.P. Flannery: *Numerical Recipes in Fortran*, 2nd ed., Cambridge University Press, New York, NY, 1992, pp. 650-59.